Unravelling long-term temporal dynamics of the invasive fruit fly *Bactrocera dorsalis* along an altitudinal gradient in Morogoro, Eastern Tanzania

Maulid W. Mwatawala[1], Joseph O. Ruboha[2], Jackline Bakengesa[3], Mwajuma K. Zinga[1], Marc De Meyer[4]

1. Department of Crop Science and Horticulture, Sokoine University of Agriculture
2. Department of Agricultural Sciences, Sokoine University of Agriculture, Mizengo Pinda Campus
3. Biology Department, Royal Museum for Central Africa, Tervuren, Belgium
4. Biology Department, The University of Dodoma, Tanzania

Corresponding author: mwatawala@sua.ac.tz

Abstract

Bactrocera dorsalis (Hendel) is the most economically important invasive fruit fly in sub-Saharan Africa, yet long-term empirical evidence linking its seasonal dynamics to environmental drivers across altitudinal gradients remains limited. We analysed 279 site-month observations of male trap catches (flies per trap per day, FTD) collected between October 2004 and February 2012 at six sites spanning 526–1,650 m above sea level along the Uluguru Mountain transect in Morogoro, Tanzania. Climatic variables (temperature, rainfall, relative humidity) were obtained from ERA5 reanalysis, and host fruit phenology was characterised for key commercial species. Abundance declined sharply with altitude, with mean FTD decreasing from 87.1 at the lowland site (SUA, 526 m) to 0.07 at the highest site (Nyandira, 1,650 m), where 55% of months recorded zero catches. Seasonal peaks occurred during the warm–wet period (November–April), but both their magnitude and duration declined with altitude, with the high season shortening from seven months at SUA to three months at Nyandira. Seasonal patterns also became less predictable at higher elevations, with the coefficient of variation of peak abundance increasing from 0.54 to 1.38. Relative humidity showed the strongest association with FTD (Spearman $\rho = 0.202$, $p = 0.0007$), while temperature showed no significant overall relationship. Host fruit availability further shaped population dynamics, with ripening of jew plum, mango, and soursop associated with increased abundance, whereas citrus and loquat had minimal influence. Overall, *B. dorsalis* abundance along the gradient is primarily structured by altitude and host availability, with climate acting as a secondary, context-dependent influence. These findings provide a clearer ecological basis for predicting pest pressure and improving management strategies across heterogeneous landscapes in East Africa.

Keywords: *Bactrocera dorsalis*, altitudinal gradient, seasonal dynamics, host phenology, population abundance, relative humidity, climatic drivers, tropical agroecosystems

Introduction

Tephritid fruit flies (Diptera: Tephritidae) rank among the most economically damaging insect pests of horticultural crops worldwide, inflicting severe pre- and post-harvest losses and constraining international trade in fresh produce [1,2]. Within this family, the oriental fruit fly, *Bactrocera dorsalis* (Hendel), stands out as a destructive invasive species whose broad host range encompasses more than 400 fruit and vegetable species [3–5]. Originally native to continental South and South-East Asia, *B. dorsalis* was first detected on the African continent along the Kenyan coast in 2003 [6]. The African populations were initially described as a separate species, *Bactrocera invadens* Drew, Tsuruta & White [7], but integrative taxonomic analyses combining morphological, molecular, and cytogenetic evidence subsequently demonstrated conspecificity, leading to formal synonymisation under *B. dorsalis* [8,9].

Following its arrival in East Africa, *B. dorsalis* spread rapidly, and by 2020 it had been recorded in more than 35 sub-Saharan countries including Indian Ocean Island nations [10]. This invasion success has been attributed to a combination of favourable tropical climates, the availability of diverse cultivated and wild host plants, and the species' competitive superiority over indigenous *Ceratitis* species [11,12]. In areas where *B. dorsalis* has established, crop losses in mango, citrus, guava, and other commercially important fruits routinely range from 30% to 80% if populations are left unmanaged [13–15], causing significant economic losses for smallholder farmers [16,17].

Across Africa, the spatial and temporal distribution of *B. dorsalis* is highly heterogeneous and strongly seasonal. Spatially, the species attains its highest densities in low- to mid-altitude agroecological zones characterised by warm temperatures and year-round host availability [1,18].

Along altitudinal gradients in East Africa, population densities decline with increasing elevation, reflecting the combined effects of cooler temperatures, reduced host diversity, and changes in landscape composition [19–21]. Temporally, populations peak during warm, humid periods that coincide with the main host fruiting seasons, declining during cooler or drier months when developmental rates slow and host resources become scarce [13,22].

Predictive distribution and ecological niche-modelling studies indicate that large areas of Africa and other tropical and subtropical regions remain climatically suitable for the establishment of *B. dorsalis* [23], and phenology-based models suggest that warming temperatures may promote seasonal expansion and year-round persistence, increasing invasion risk in temperate fruit-growing regions under future climate scenarios [24,25]. Understanding how environmental drivers interact to shape population dynamics across heterogeneous landscapes is therefore essential for developing climate-sensitive surveillance and evidence-based integrated pest management (IPM) strategies.

Previous studies on the ecology of *B. dorsalis* in Tanzania documented its host utilisation, seasonality, competitive interactions with native fruit flies, and progressive dominance along an altitudinal transect in Morogoro [13,19,20,26]. However, these investigations were generally limited in temporal scope, typically spanning one to three years, and did not examine long-term population dynamics in relation to host fruit phenology, landscape-level host availability, and the full altitudinal gradient simultaneously. Long-term datasets are critical for distinguishing persistent ecological signals from short-term variability and for strengthening the evidence base on which surveillance and management decisions rest [1,10].

The present study addresses this gap by analysing *B. dorsalis* population dynamics over a seven-year period (October 2004 to February 2012) across six trapping sites spanning 526 to 1,650 m

above sea level along the eastern slopes of the Uluguru Mountains, Morogoro Region, Tanzania. We hypothesised that: (i) abundance declines with increasing altitude, reflecting thermal constraints and reduced host availability; (ii) seasonal population peaks are stronger and longer at lower elevations; (iii) moisture-related climatic variables, particularly relative humidity, are more strongly associated with abundance than temperature alone; and (iv) the timing and availability of preferred host fruits contribute substantially to local population increases. By integrating long-term trapping data with ERA5 climate reanalysis products, host fruit phenology records, and both parametric and machine learning analytical approaches, this study aims to provide a comprehensive ecological characterisation of *B. dorsalis* population dynamics along a tropical altitudinal gradient and to inform targeted, landscape-specific management strategies.

Methodology

Study area and agroecological zones

Monitoring of *B. dorsalis* was carried out in Morogoro Region, eastern–central Tanzania, along an altitudinal gradient on the eastern slopes of the Uluguru Mountains. Sites were selected to represent four agroecological zones following the classification systems described for the Eastern Arc Mountains [27,28]. This zonation reflects distinct changes in cropping systems, host plant composition, and climatic regimes along the transect.

Fig 1. 3D elevation surface around the six monitoring localities (SRTM DEM), highlighting the lowland–highland gradient.

A preliminary analysis revealed a strong negative correlation between altitude and temperature (Spearman's $\rho = -0.79$), consistent with the well-documented adiabatic lapse rate in tropical

mountains. To reduce collinearity in subsequent analyses, agroecological zone was retained as a categorical landscape variable while preserving the ecological meaning of the altitudinal gradient [29].

The lowland agro-mosaic (below ~600 m a.s.l.) encompassed two sites: SUA (526 m) and Mlali (581 m), characterised by warm agricultural landscapes with diverse tropical fruit production, including citrus (*Citrus sinensis* (L.) Osbeck, *C. limon* (L.) Osbeck, *C. reticulata* Blanco), mango (*Mangifera indica* L.), guava (*Psidium guajava* L.), jew plum (*Spondias cytherea* Sonn.), and soursop (*Annona muricata* L.). The mid-elevation transition zone contained one site, Kibundi (843 m), in a mixed smallholder landscape dominated by banana (*Musa* spp.), avocado (*Persea americana* Mill.), maize, and beans. The sub-montane farming zone included two sites: Langali (1,105 m) and Visada (1,302 m), where staple crops predominated and tropical fruit trees were relatively sparse. Finally, the montane agroforestry zone was represented by Nyandira (1,650 m), a cooler landscape dominated by temperate fruit crops such as apple (*Malus domestica* Borkh.), peach (*Prunus persica* (L.) Batsch), and plum (*Prunus salicina* Lindl.), often intercropped with coffee (*Coffea canephora* Pierre ex A. Froehner).

Sampling design and Trap deployment

Six monitoring sites, spanning approximately 500 to 1,650 m a.s.l., were established along the gradient. Monitoring commenced in October 2004 at the two altitudinal extremes, SUA (lowland) and Nyandira (montane), with routine monitoring at SUA beginning in October 2005 following an initial pilot phase. In October 2008, the network was expanded to include Mlali, Kibundi, Langali, and Visada, and all six sites were monitored continuously until February 2012.

Adult male *B. dorsalis* were monitored using modified McPhail traps baited with methyl eugenol (ME; Scentry Cie, Billings, MT, USA), a highly effective male-specific parapheromone widely used in tephritid surveillance programmes [31,32]. Methyl eugenol attracts *B. dorsalis* from the surrounding landscape, thereby enabling sampling at a broader spatial scale. Traps were fitted with dichlorvos (DDVP) strips as a killing agent and suspended approximately 2 m above ground level within the host tree canopy. Across all sites, inter-trap spacing was maintained at a minimum of 1,000 m to ensure spatial independence of catches.

At SUA, traps were initially placed in mango (cv. Dodo), citrus (cv. Sweet Seedling), and guava trees, later expanded to five traps with additional placements in mango (cv. Sindano Nyeusi) and citrus (cv. Tahiti lime). At Nyandira, traps were installed in peach and plum trees. At the four intermediate sites, three replicate traps per site were placed predominantly in mango trees. After each sampling event, traps were randomly repositioned within the sampling area to minimise location bias. Lure plugs and DDVP strips were replaced at approximately monthly intervals to maintain trapping efficiency.

Sampling procedures followed established protocols for tephritid monitoring in East Africa [13,19]. Collected specimens were transported to the SUA Entomology Laboratory, where they were sorted and identified using standard morphological keys [2,34] and confirmed with the integrative diagnostic tools of Virgilio et al. [33]. Specimens previously identified as *Bactrocera invadens* were treated as *B. dorsalis* following formal synonymisation based on integrative taxonomic evidence [8,9].

Fruit phenology data

Phenological data for major host fruit species were obtained from the systematic weekly observations of Shechambo [30], conducted at the SUA Horticultural Unit. Representative host species selected for analysis included mango, citrus, guava, soursop, loquat (*Eriobotrya japonica* (Thunb.) Lindl.), jew plum, and strawberry guava (*Psidium cattleianum* Sabine). These species were chosen on the basis of their documented high incidence and infestation rates for *B. dorsalis* in the study area [19,20,26].

Phenological stages recorded included flowering, fruit set, immature fruit, mature fruit, and ripe fruit. For subsequent analyses, periods of host fruit availability (i.e., presence of mature and ripe fruit) were coded as binary indicators for each host species and calendar month (S1 Fig).

Weather data collection

Monthly climatic variables; mean air temperature (°C), total rainfall (mm), and mean relative humidity (%) were compiled for each monitoring site. At SUA, primary data were obtained from the Tanzania Meteorological Authority (TMA) and supplemented with on-site temperature records from iButton data loggers. At Nyandira, temperature was recorded with iButton loggers, while rainfall data were derived from gridded climate products.

To ensure temporal continuity across all sites and fill observational gaps, additional climatic data were extracted from the ERA5 global reanalysis [36], accessed via Google Earth Engine [37]. Site-level baseline climate was further characterised using bioclimatic variables (bio01–bio19) from WorldClim version 2.1 at 30-arc-second resolution [35]. ERA5 and WorldClim data supplemented, but did not replace, direct observations where these were available.

For analytical consistency, daily records were aggregated into monthly means (temperature, relative humidity) and monthly totals (rainfall). These three climatic variables were selected on the basis of their established influence on the development, survival, reproduction, and dispersal of *B. dorsalis* [14,38].

Abundance index and temporal aggregation

Fruit fly abundance was expressed as flies per trap per day (FTD), the standard index recommended for tephritid population monitoring [31]. For each inspection interval *i*, FTD was calculated as:

$$FTD_i = C_i / (T_i \times D_i)$$

where C_i is the total number of *B. dorsalis* captured, T_i is the number of traps deployed, and D_i is the number of days since the previous inspection. Monthly mean FTD for a given calendar month *m* was then calculated as a trap-day weighted mean, i.e., the total flies attributed to month *m* divided by the total trap-days in that month. When inspection intervals spanned two calendar months, catches were allocated proportionally based on the number of days in each month, assuming a constant daily catch rate. Monthly uncertainty was summarised as the weighted standard error of inspection-interval FTD values, with asymmetric clipping at zero to prevent negative lower bounds.

Data analysis

Fruit fly abundance was expressed as flies per trap per day (FTD) and log-transformed using $\log_{10}(1 + x)$ prior to analysis [39]. Seasonal variation was assessed using the Kruskal–Wallis test [40]. Associations between FTD and climatic variables were quantified using Spearman's rank

correlation [41], chosen for its robustness to the skewed, non-linear relationships characteristic of count data.

To model climate–abundance relationships while accounting for overdispersion, generalised linear models (GLMs) with a negative binomial error distribution and log link function were fitted [42,43]. Two models were compared: a climate-only model and a full model incorporating locality as a proxy for agroecological zone. Within-site temporal correlation was addressed using generalised estimating equations (GEE) with an exchangeable correlation structure [44]. Model effects were expressed as incidence rate ratios (IRR) with 95% Wald confidence intervals, and model selection was guided by Akaike's Information Criterion.

To capture non-linear relationships and interactions among predictors, three ensemble machine learning algorithms were applied: LightGBM with Tweedie loss (p = 1.9) [45], Random Forest [46], and Gradient Boosting [47]. The Tweedie loss was selected because it accommodates the semi-continuous, zero-inflated distribution of FTD. Model performance was evaluated using year-blocked GroupKFold cross-validation to prevent temporal leakage [47]. Predictor importance was quantified using SHapley Additive exPlanations (SHAP) [48], which assigns each feature an importance value grounded in cooperative game theory. From the SHAP output, mean absolute SHAP values provided global predictor rankings, dependence plots revealed non-linear predictor–response relationships, and interaction analyses examined the altitude–mango ripening interaction. A predictor evidence summary integrated SHAP importance with univariate statistical tests (Spearman's ρ for continuous, Mann–Whitney U for binary, and Kruskal–Wallis H for categorical predictors), with p-values corrected using the Benjamini–Hochberg false discovery rate procedure [49].

All analyses were performed in Python 3.13.5 using pandas [50], NumPy [51], scikit-learn [47], LightGBM [45], SHAP [48], statsmodels [52], and SciPy [53]. Statistical significance was assessed at $\alpha = 0.05$ throughout.

Results

Temporal dynamics and altitudinal gradient in abundance

Monthly FTD varied markedly across the six sites, reflecting a pronounced altitudinal gradient in *B. dorsalis* abundance (Fig 2). At the lowland SUA site (526 m a.s.l.), FTD fluctuated between approximately 10 and 250 flies trap^{-1} day^{-1} throughout the study period, with recurrent peaks during the warm, wet months (November–April) and troughs during the cool, dry season (May–October). The adjacent lowland site of Mlali (581 m) showed a similar seasonal pattern but at lower absolute densities (mean FTD = 38.9). At the mid-elevation site of Kibundi (843 m), FTD was further reduced (mean = 22.3), and seasonal peaks rarely exceeded 100 flies trap^{-1} day^{-1}. At Langali (1,105 m), representing the sub-montane transition zone, mean FTD declined to 2.2, with only sporadic increases above 5 flies trap^{-1} day^{-1}. At the two highest sites, Visada (1,302 m) and Nyandira (1,650 m), abundance was extremely low (mean FTD = 0.19 and 0.07, respectively), with Nyandira recording zero catches in 55% of all months monitored (Fig 1).

Fig 2. Monthly temporal dynamics of *B. dorsalis* FTD at six sites along the Mount Uluguru transect, Morogoro Region, Tanzania, 2004–2012. Sites are arranged from lowest (SUA, 526 m, top) to highest elevation (Nyandira, 1,650 m, bottom). Points show monthly mean FTD ± SEM.

Seasonal phenology across the gradient

Seasonal boxplots of monthly FTD at each site (Fig 3) showed that the lowland SUA site exhibited the most pronounced and statistically significant monthly variation (Kruskal–Wallis, $p < 0.001$), with the highest median FTD in January (114.9) and the lowest in September (18.7). At the montane Nyandira site, monthly variation was also significant ($p = 0.037$), driven by elevated FTD in January–March and near-zero values from May to November. In contrast, at the intermediate sites of Mlali, Kibundi, and Langali, Kruskal–Wallis tests were not significant ($p = 0.114$, 0.085, and 0.195, respectively), indicating weaker seasonal structure relative to interannual variability. Similarly, no significant monthly variation was detected at Visada ($p = 0.117$).

Fig 3. Seasonal phenology of *B. dorsalis* across the altitudinal gradient. (A) Monthly FTD boxplots by site with Kruskal–Wallis test p-values.

Seasonal predictability metrics (Fig 4) described three aspects of how the population changes across the gradient. First, seasonal amplitude (the difference between the highest and lowest monthly FTD) decreased sharply with altitude, from 96.2 at SUA to 0.2 at Nyandira (Fig 4A). Second, the coefficient of variation (CV) of peak-month FTD increased with altitude, from 0.54 at SUA to 1.38 at Nyandira (Fig 4B), showing that seasonal peaks became less predictable at higher elevations. Third, the duration of the high season (months when FTD was above the site's annual average) ranged from seven months at SUA to only three months at Nyandira (Fig 4C).

Fig 4. Seasonal predictability metrics: (A) amplitude (peak–trough FTD) versus altitude; (B) coefficient of variation of peak-month FTD; (C) duration of the high season at each site.

Seasonal effects from negative binomial GLMs

The negative binomial models (Fig 5) confirmed the seasonal pattern observed above. At SUA (526 m), FTD was significantly lower than in January from April to December, with the largest reductions in September (about −80%) and October (−70%). At Mlali and Kibundi, FTD decreased by 60–90% from April to November. At the three highest sites, FTD was also lower than in January in most months, although overall levels were already very low.

Fig 5. Seasonal effects on *B. dorsalis* FTD from negative binomial GLMs. (A) Percentage change in FTD for each month relative to January (reference) at all six sites. Green bars indicate significant departures ($p < 0.05$); beige bars are non-significant.

Annotated seasonal bar charts (Fig 6) showed that population peaks occurred consistently during the early warm–wet season (January at most sites), with minor secondary peaks at Langali and Visada in September. The contrast between peak and low periods increased sharply with altitude, indicating that populations at higher elevations are concentrated into a much shorter seasonal window.

Fig 6. Monthly mean FTD (± SEM) at each site with peak and trough months annotated. Red shading indicates months above the site-specific annual mean.

Effects of climatic variables on abundance

Bivariate relationships between FTD and climate variables (Fig 7) showed that relative humidity had the strongest positive association with FTD (Spearman $\rho = 0.202$, $p = 0.0007$), followed by rainfall ($\rho = 0.119$, $p = 0.046$). Temperature showed no significant overall relationship ($\rho = -0.084$, $p = 0.162$).

The correlation matrices (Fig 8) showed that rainfall and relative humidity were strongly correlated with each other ($\rho = 0.75$, $p < 0.001$), indicating that they represent similar seasonal moisture conditions.

Fig 7. Effects of climatic variables on *B. dorsalis* FTD: Bivariate scatter plots of FTD against temperature, rainfall, and relative humidity with LOESS trend lines and Spearman ρ values. Points are coloured by site.

Fig 8. Effects of climatic variables on *B. dorsalis* FTD: Multivariate Pearson (left) and Spearman (right) correlation matrices across all sites combined.

Site-specific correlations (S2 Fig) showed that these relationships were strongest at the lowland sites. The association between FTD and relative humidity was highest at SUA ($\rho = 0.55$, $p < 0.001$), Mlali ($\rho = 0.50$, $p < 0.01$), and Kibundi ($\rho = 0.55$, $p < 0.001$). Rainfall also showed significant positive relationships with FTD at these sites (SUA: $\rho = 0.47$, $p < 0.001$; Mlali: $\rho = 0.42$, $p < 0.01$; Kibundi: $\rho = 0.50$, $p < 0.01$). In contrast, no significant relationships were observed at the higher-elevation sites (Langali, Visada, Nyandira), where overall abundance was low.

Host fruit phenology and abundance

The SHAP analysis of host fruit ripening (Fig 9) showed that not all host fruits contributed equally to *B. dorsalis* abundance. Ripening of jew plum (*Spondias cytherea*) had the strongest positive effect on FTD (SHAP difference = +1.221). Soursop (*Annona muricata*) and mango (*Mangifera indica*) also increased FTD, but to a lesser extent (+0.275 and +0.159, respectively). In contrast, citrus and loquat had little to no effect, with slightly negative contributions (−0.022 and −0.055), indicating that their presence did not meaningfully increase local populations.

Fig 9. Host phenology effects on *B. dorsalis* abundance. SHAP difference (ripe minus not-ripe) for five host fruits, indicating the contribution of each host's ripening to predicted FTD.

The altitude–mango interaction (Fig 10) showed that the effect of altitude on FTD depended on host availability. At lower elevations, where mango was present and ripening between January and March, altitude contributed positively to FTD (mean SHAP = +3.07 at SUA and +2.17 at Mlali). At mid-elevation (Langali), the effect was close to zero (−0.22), while at higher elevations (Visada and Nyandira), where mango was absent, altitude had a strong negative effect (−1.92 and −8.43, respectively).

Fig 10. Host phenology effects on *B. dorsalis* abundance. SHAP value for altitude stratified by mango ripening status, showing the altitude–mango interaction.

Overall, the negative effect of altitude became stronger above about 1,100 m, especially where key host fruits such as mango were no longer present. This pattern was consistent across seasons, although small differences were observed between months when mango was ripe and when it was not. The phenological calendar (S1 Fig) showed that mango ripening (December–May) at the lower sites coincided with the main period of *B. dorsalis* activity.

Key drivers of B. dorsalis abundance

Across all analyses, including the machine learning model used to assess predictor importance, a consistent pattern emerged in the factors shaping *B. dorsalis* abundance along the altitudinal gradient (Fig 11). Altitude was the primary factor, with abundance declining sharply at higher elevations. This decline was accompanied by weaker seasonality, reduced predictability, and shorter periods of population activity.

Fig 11. Machine learning predictor importance. (A) Mean absolute SHAP values ranking all 20 predictors by their contribution to FTD prediction.

Host fruit availability further shaped these patterns (Fig 12). The presence and ripening of key host fruits, particularly jew plum and mango, were associated with higher FTD, while sites lacking these hosts—especially at higher elevations—supported only low and sporadic populations.

Fig 12. Machine learning predictor importance. Predictor evidence summary integrating SHAP importance (x-axis, lollipop length) with the type and FDR-adjusted significance of univariate statistical tests (point colour and size).

Climatic conditions also influenced abundance, with relative humidity showing the strongest and most consistent relationship with FTD. However, these effects were most evident at lower elevations, where populations were well established, and were weak or absent at higher elevations. Together, these results show that *B. dorsalis* abundance along the gradient is primarily structured by altitude and host availability, with climate acting as a secondary, context-dependent influence.

Discussion

This long-term study demonstrates that *B. dorsalis* populations exhibit pronounced seasonal dynamics, with consistent peaks during the warm–wet season and declines during the cool-dry period. Such rainfall-driven seasonality, which regulates host availability, is widely reported across tropical systems, including Tanzania [13], Kenya [38], Benin [18], Cameroon [22], and Asia [54,55], indicating a broadly conserved temporal structure. More broadly, the ecology and spread of *B. dorsalis* across Africa reflect interacting effects of climate, host availability, and landscape structure [10]. However, the long-term data further show that seasonal dynamics are not

uniform across environments. Along the altitudinal gradient, population peaks became progressively shorter, weaker, and less predictable at higher elevations. This pattern indicates that while lowland populations follow relatively stable climatic and phenological cycles, highland populations are more constrained and temporally variable. Our study has refined seasonal understanding by resolving the timing and reliability of peak and low population periods across years, which is important for anticipating periods of highest risk.

Our results showed a clear decline in abundance with increasing elevation, demonstrating the important role of altitude in structuring populations. This widespread pattern indicates that altitude imposes fundamental constraints on population persistence. While lower temperatures at higher elevations are known to slow development and reduce reproductive performance [14,56,57], the present study shows that these effects are compounded by host limitation. The marked decline in abundance above mid-elevations coincided with the absence of key hosts, and interaction analyses showed that altitude effects were strongly mediated by host availability, consistent with observations in Cameroon [22]. Similar patterns have been documented along the Morogoro transect in Tanzania [19,20], across East Africa [21], and in southern Africa [64], as well as across ecological zones in India [69]. Species distribution modelling studies further show that climatic suitability, including temperature gradients associated with elevation, strongly determines the geographic range of *B. dorsalis* [58]. In particular, phenology-based models incorporating environmental gradients have reported how temperature and moisture jointly shape its potential distribution across regions [23].

Climatic influences on abundance were dominated by moisture-related variables, with relative humidity and rainfall showing stronger associations than temperature. This pattern is consistent with established mechanisms, where adequate moisture improves survival, pupation conditions,

and host fruit quality [14,38]. In Benin, infestation levels reflect combined effects of abiotic conditions and host factors [15], while broader studies demonstrate that climate operates in conjunction with landscape and season to regulate population dynamics [64]. Thermal biology studies have reported the role of temperature in shaping seasonal abundance [65]. Overall, these findings indicate that moisture acts as a proximate driver of seasonal population fluctuations within suitable environments, whereas temperature and host distribution define broader spatial limits.

Host fruit availability emerged as a key driver of population dynamics, with a small number of hosts contributing disproportionately to population increases. The strong influence of jew plum highlights the importance of non-commercial hosts in sustaining populations between major cropping periods, consistent with the recognised role of *Spondias* species as preferred hosts [3]. Similar phenological linkages have been reported elsewhere, including in Uganda, where population peaks track mango fruiting cycles [59], and in Senegal, where fruiting stages influence oviposition behaviour [60]. Host suitability also varies with fruit ripening stage, influencing infestation potential [61], while seasonal host availability and diversity further regulate population dynamics [62].

Mango remains a primary host in East Africa [1,26], although its influence is partly mediated by favourable climatic conditions at low elevations. In contrast, citrus contributes little to population growth under natural conditions. Host prioritisation studies further confirm that reproductive success varies significantly among host plants [63]. Importantly, host availability interacts with altitude to shape population patterns. The absence of key hosts at higher elevations amplifies the decline in abundance, reinforcing the need to consider host distribution alongside climatic gradients. By isolating the role of key host fruits, this study clarifies how resource availability drives population build-up, which is important for targeting host-based management strategies.

The observed patterns provide a basis for improving surveillance and management strategies. Altitude offers a practical framework for risk stratification, with lowland areas experiencing consistently higher and more predictable pest pressure. In these environments, climate-informed forecasting—particularly using rainfall and humidity indicators—can improve the timing of interventions such as bait sprays and male annihilation [18,66]. Similar approaches have proven effective in Sri Lanka using time-series models [55]. At higher elevations, reduced predictability of population peaks suggests that fixed seasonal calendars are less effective, and adaptive monitoring based on trap thresholds is more appropriate. Integrating host phenology with climate-based forecasts could further enhance early warning systems. In island systems, invasion dynamics and niche interactions further illustrate the role of landscape structure [67].

This study is based on male trap captures, which do not directly reflect female oviposition or infestation levels. Incorporating fruit sampling would improve inference on crop damage. In addition, unequal sampling periods and site-specific phenological data may limit comparability across the gradient. Finally, unmeasured biotic factors such as parasitism, competition, and management practices may also influence population dynamics [11,68].

Conclusion

Long-term monitoring revealed consistent seasonal dynamics and strong altitudinal structuring of *B. dorsalis* populations. Lowland populations exhibited predictable peaks, whereas highland populations remained low and irregular. These patterns reflect interacting effects of climate, host phenology, and landscape context, underscoring the importance of long-term data for developing predictive and adaptive pest management strategies. These findings support the use of long-term, climate-informed monitoring systems to improve the timing and targeting of *B. dorsalis*

management. In lowland areas, where populations are consistently high and seasonally predictable, interventions should be synchronised with rainfall patterns and host fruit phenology to maximise effectiveness. In contrast, highland systems require adaptive, threshold-based monitoring due to lower and less predictable population dynamics. Integrating host phenology, climatic indicators, and spatial risk stratification into early warning systems will enhance decision-making and support more efficient, landscape-level pest management strategies.

Author's contributions

Maulid W. Mwatawala (MWM): Conceptualization, Methodology, Investigation, Data Collection, Writing-original draft.

Marc De Meyer (MDM): Methodology, Resources, Data Collection, Writing-review & editing.

Jackline Bakengesa (JB) and Mwajuma Zinga (MW): Writing-review & editing.

Joseph O Ruboha (JOR): Formal analysis, Writing-review & editing

Ethics

The research was conducted from 2004 and 2012, before the establishment of formal ethical review boards. The study involved only insect sampling and environmental observations and did not involve human participants or vertebrate animals. All procedures complied with institutional guidelines and accepted scientific practices applicable at the time of the study.

Acknowledgements

The study was carried out in several phases between 2004 and 2012 and was supported by multiple funding sources, including the Belgian Development Cooperation through the Framework Programme with the Royal Museum for Central Africa (Projects F13 and S1_TNZ_IPM), the joint

Food and Agriculture Organization / International Atomic Energy Agency (FAO/IAEA) Programme on Nuclear Techniques in Food and Agriculture through the Coordinated Research Project *"Resolution of Cryptic Species Complexes of Tephritid Pests to Overcome Constraints to the Sterile Insect Technique (SIT) Application and International Trade"*, the International Foundation of Science (Project C3956), and the Belgian Science Policy (Project MO/37/017).

Declaration

Artificial intelligence (AI) tools were used solely for grammar checking, spelling correction, and improving language clarity. All analyses, interpretations, and scientific conclusions were conducted entirely by the authors.

Conflict of interest

The authors declare that there is NO conflict of interest regarding the publication of this Manuscript.

References

1. Ekesi S, De Meyer M, Mohamed SA, Virgilio M, Borgemeister C. Taxonomy, Ecology, and Management of Native and Exotic Fruit Fly Species in Africa. Annu Rev Entomol. 2016;61: 219–238. doi:10.1146/annurev-ento-010715-023603
2. White I, Elson-Harris M. Fruit Flies of Economic Significance: Their Identification and Bionomics. Wallingford: CAB International; 1992. doi:10.1079/9780851987903.0000
3. Allwood AJ, Chinajariyawong A, Drew RAI, Hamacek EL, Hancock DL, Hengsawad C, et al. Host plant records for fruit flies (Diptera: Tephritidae) in Southeast Asia. Raffles Bull Zool. 1999;47(7): 1–102.
4. Clarke AR, Armstrong KF, Carmichael AE, Milne JR, Raghu S, Roderick GK, et al. Invasive phytophagous pests arising through a recent tropical evolutionary radiation: the Bactrocera dorsalis complex of fruit flies. Annu Rev Entomol. 2005;50: 293–319. doi:10.1146/ANNUREV.ENTO.50.071803.130428
5. Leblanc L, Hossain MA, Khan SA, San Jose M, Rubinoff D. A Preliminary Survey of the Fruit Flies (Diptera: Tephritidae: Dacinae) of Bangladesh. Proc Hawaiian Entomol Soc. 2013;45: 51–58.
6. Lux SA, Copeland RS, White IM, Manrakhan A, Billah MK. A New Invasive Fruit Fly Species from the Bactrocera dorsalis (Hendel) Group Detected in East Africa. Int J Trop Insect Sci. 2003;23(4): 355–361. doi:10.1017/S174275840001242X
7. Drew RAI, Tsuruta K, White IM. A new species of pest fruit fly (Diptera: Tephritidae: Dacinae) from Sri Lanka and Africa. Afr Entomol. 2005;13(1): 149–154.
8. Schutze MK, Mahmood K, Pavasovic A, Bo W, Newman J, Clarke AR, et al. One and the same: Integrative taxonomic evidence that Bactrocera invadens (Diptera: Tephritidae) is

the same species as the Oriental fruit fly Bactrocera dorsalis. Syst Entomol. 2015;40(2): 472–486. doi:10.1111/SYEN.12114

9. Schutze MK, Aketarawong N, Amornsak W, Armstrong KF, Augustinos AA, Barr N, et al. Synonymization of key pest species within the Bactrocera dorsalis species complex (Diptera: Tephritidae). Syst Entomol. 2015;40(2): 456–471. doi:10.1111/SYEN.12113
10. Mutamiswa R, Nyamukondiwa C, Chikowore G, Chidawanyika F. Overview of oriental fruit fly, Bactrocera dorsalis (Hendel) (Diptera: Tephritidae) in Africa: From invasion, bio-ecology to sustainable management. Crop Prot. 2021;141: 105492. doi:10.1016/J.CROPRO.2020.105492
11. Ekesi S, Billah MK, Nderitu PW, Lux SA, Rwomushana I. Evidence for competitive displacement of Ceratitis cosyra by Bactrocera invadens. Bull Entomol Res. 2009;99(2): 153–161.
12. Rwomushana I, Ekesi S, Ogol CKPO, Gordon I. Mechanisms contributing to the competitive success of the invasive fruit fly Bactrocera invadens over the indigenous mango fruit fly, Ceratitis cosyra. Entomol Exp Appl. 2009;133(1): 27–37. doi:10.1111/J.1570-7458.2009.00897.X
13. Mwatawala MW, De Meyer M, Makundi RH, Maerere AP. Seasonality and host utilization of the invasive fruit fly, Bactrocera invadens (Dipt., Tephritidae) in central Tanzania. J Appl Entomol. 2006;130(9–10): 530–537. doi:10.1111/J.1439-0418.2006.01099.X
14. Rwomushana I, Ekesi S, Ogol CKPO, Gordon I. Effect of temperature on development and survival of immature stages of Bactrocera invadens (Diptera: Tephritidae). J Appl Entomol. 2008;132(9–10): 832–839. doi:10.1111/J.1439-0418.2008.01318.X

15. Vayssières JF, Korie S, Ayegnon D. Correlation of fruit fly (Diptera Tephritidae) infestation of major mango cultivars in Borgou (Benin) with abiotic and biotic factors and assessment of damage. Crop Prot. 2009;28(6): 477–488. doi:10.1016/J.CROPRO.2009.01.010
16. Badii KB, Billah MK, Afreh Nuamah K, Obeng Ofori D, Nyarko G. Review of the pest status, economic impact and management of fruit-infesting flies (Diptera: Tephritidae) in Africa. Afr J Agric Res. 2015;10(12): 1488–1498. doi:10.5897/AJAR2014.9278
17. Muriithi BW, Diiro GM, Affognon H, Ekesi S. Economic impact of integrated pest management strategies for the suppression of mango-infesting fruit fly species in Africa. In: Ekesi S, Mohamed SA, De Meyer M, editors. Fruit Fly Research and Development in Africa. Cham: Springer; 2016. pp. 755–770. doi:10.1007/978-3-319-43226-7_33
18. Vayssières JF, De Meyer M, Ouagoussounon I, Sinzogan A, Adandonon A, Korie S, et al. Seasonal Abundance of Mango Fruit Flies (Diptera: Tephritidae) and Ecological Implications for Their Management in Mango and Cashew Orchards in Benin. J Econ Entomol. 2015;108(5): 2213–2230. doi:10.1093/jee/tov143
19. Geurts K, Mwatawala M, Meyer M De. Indigenous and Invasive Fruit Fly Diversity along an Altitudinal Transect in Eastern Central Tanzania. J Insect Sci. 2012;12: 12. doi:10.1673/031.012.1201
20. Geurts K, Mwatawala MW, De Meyer M. Dominance of an invasive fruit fly species, Bactrocera invadens, along an altitudinal transect in Morogoro, Eastern Central Tanzania. Bull Entomol Res. 2014;104(3): 288–294. doi:10.1017/S0007485313000722
21. Odanga JJ, Mohamed S, Mwalusepo S, Olubayo F, Nyankanga R, Khamis F, et al. Spatial Distribution of Bactrocera dorsalis and Thaumatotibia leucotreta in Smallholder Avocado

Orchards along Altitudinal Gradient of Taita Hills and Mount Kilimanjaro. Insects. 2018;9(2): 71. doi:10.3390/INSECTS9020071

22. Nanga Nanga S, Hanna R, Fotso Kuate A, Fiaboe KKM, Nchoutnji I, Ndjab M, et al. Tephritid Fruit Fly Species Composition, Seasonality, and Fruit Infestations in Two Central African Agro-Ecological Zones. Insects. 2022;13(11): 1045. doi:10.3390/insects13111045
23. De Villiers M, Hattingh V, Kriticos DJ, Brunel S, Vayssières JF, Sinzogan A, et al. The potential distribution of Bactrocera dorsalis: Considering phenology and irrigation patterns. Bull Entomol Res. 2016;106(1): 19–33. doi:10.1017/S0007485315000693
24. Liu H, Zhang DJ, Xu YJ, Wang L, Cheng DF, Qi YX, et al. Invasion, expansion, and control of Bactrocera dorsalis (Hendel) in China. J Integr Agric. 2019;18(4): 771–787. doi:10.1016/S2095-3119(18)62015-5
25. Stephens AEA, Kriticos DJ, Leriche A. The current and future potential geographical distribution of the oriental fruit fly, Bactrocera dorsalis (Diptera: Tephritidae). Bull Entomol Res. 2007;97(4): 369–378. doi:10.1017/S0007485307005044
26. Mwatawala MW, De Meyer M, Makundi RH, Maerere AP. Host range and distribution of fruit-infesting pestiferous fruit flies (Diptera, Tephritidae) in selected areas of Central Tanzania. Bull Entomol Res. 2009;99(6): 629–641. doi:10.1017/S0007485309006695
27. Burgess ND, Butynski TM, Cordeiro NJ, Doggart NH, Fjeldså J, Howell KM, et al. The biological importance of the Eastern Arc Mountains of Tanzania and Kenya. Biol Conserv. 2007;134(2): 209–231. doi:10.1016/j.biocon.2006.08.015
28. Lovett J, Wasser SK, editors. Biogeography and Ecology of the Rain Forests of Eastern Africa. Cambridge: Cambridge University Press; 1993.

29. Zuur AF, Ieno EN, Walker NJ, Saveliev AA, Smith GM. Mixed Effects Models and Extensions in Ecology with R. New York: Springer; 2009. doi:10.1007/978-0-387-87458-6

30. Shechambo L. Effects of host availability on seasonal abundance of the fruit fly Bactrocera invadens Drew, Tsuruta & White in Morogoro [dissertation]. Morogoro: Sokoine University of Agriculture; 2008.

31. FAO/IAEA. Trapping guidelines for area-wide fruit fly programmes. Enkerlin WR, Reyes-Flores J, editors. 2nd ed. Vienna: IAEA; 2018.

32. Tan KH, Nishida R. Methyl Eugenol: Its Occurrence, Distribution, and Role in Nature, Especially in Relation to Insect Behavior and Pollination. J Insect Sci. 2012;12: 56. doi:10.1673/031.012.5601

33. Virgilio M, Jordaens K, Breman FC, Backeljau T, de Meyer M. Identifying Insects with Incomplete DNA Barcode Libraries, African Fruit Flies (Diptera: Tephritidae) as a Test Case. PLoS ONE. 2012;7(2): e31581. doi:10.1371/JOURNAL.PONE.0031581

34. Virgilio M, White I, De Meyer M. A set of multi-entry identification keys to African frugivorous flies (Diptera, Tephritidae). ZooKeys. 2014;428: 97–108. doi:10.3897/zookeys.428.7366

35. Fick SE, Hijmans RJ. WorldClim 2: new 1-km spatial resolution climate surfaces for global land areas. Int J Climatol. 2017;37(12): 4302–4315. doi:10.1002/JOC.5086

36. Hersbach H, Bell B, Berrisford P, Hirahara S, Horányi A, Muñoz-Sabater J, et al. The ERA5 global reanalysis. Q J R Meteorol Soc. 2020;146(730): 1999–2049. doi:10.1002/QJ.3803

546 37. Gorelick N, Hancher M, Dixon M, Ilyushchenko S, Thau D, Moore R. Google Earth
547 Engine: Planetary-scale geospatial analysis for everyone. Remote Sens Environ. 2017;202:
548 18–27. doi:10.1016/J.RSE.2017.06.031
549 38. Ekesi S, Nderitu PW, Rwomushana I. Field infestation, life history and demographic
550 parameters of the fruit fly Bactrocera invadens (Diptera: Tephritidae) in Africa. Bull
551 Entomol Res. 2006;96(4): 379–386.
552 39. Zar JH. Biostatistical Analysis. 5th ed. Upper Saddle River: Pearson Prentice Hall; 2010.
553 40. Kruskal WH, Wallis WA. Use of Ranks in One-Criterion Variance Analysis. J Am Stat
554 Assoc. 1952;47(260): 583–621. doi:10.1080/01621459.1952.10483441
555 41. Spearman C. The Proof and Measurement of Association between Two Things. Am J
556 Psychol. 1904;15(1): 72. doi:10.2307/1412159
557 42. Cameron AC, Trivedi PK. Regression Analysis of Count Data. 2nd ed. Cambridge:
558 Cambridge University Press; 2013. doi:10.1017/CBO9781139013567
559 43. Hilbe JM. Negative Binomial Regression. 2nd ed. Cambridge: Cambridge University Press;
560 2011. doi:10.1017/CBO9780511973420
561 44. Liang KY, Zeger SL. Longitudinal data analysis using generalized linear models.
562 Biometrika. 1986;73(1): 13–22. doi:10.1093/BIOMET/73.1.13
563 45. Ke G, Meng Q, Finley T, Wang T, Chen W, Ma W, et al. LightGBM: A Highly Efficient
564 Gradient Boosting Decision Tree. In: Guyon I, Von Luxburg U, Bengio S, Wallach H,
565 Fergus R, Vishwanathan S, et al., editors. Advances in Neural Information Processing
566 Systems. Vol. 30. 2017. pp. 3146–3154.
567 46. Breiman L. Random forests. Mach Learn. 2001;45(1): 5–32.
568 doi:10.1023/A:1010933404324

569 47. Pedregosa F, Varoquaux G, Gramfort A, Michel V, Thirion B, Grisel O, et al. Scikit-learn:
570 Machine Learning in Python. J Mach Learn Res. 2011;12: 2825–2830.
571 48. Lundberg SM, Lee SI. A Unified Approach to Interpreting Model Predictions. In: Guyon
572 I, Von Luxburg U, Bengio S, Wallach H, Fergus R, Vishwanathan S, et al., editors.
573 Advances in Neural Information Processing Systems. Vol. 30. 2017. pp. 4766–4775.
574 49. Benjamini Y, Hochberg Y. Controlling the False Discovery Rate: A Practical and Powerful
575 Approach to Multiple Testing. J R Stat Soc Ser B. 1995;57(1): 289–300.
576 doi:10.1111/J.2517-6161.1995.TB02031.X
577 50. McKinney W. Data Structures for Statistical Computing in Python. Proc 9th Python Sci
578 Conf. 2010;445(1): 56–61. doi:10.25080/majora-92bf1922-00a
579 51. Harris CR, Millman KJ, van der Walt SJ, Gommers R, Virtanen P, Cournapeau D, et al.
580 Array programming with NumPy. Nature. 2020;585(7825): 357–362. doi:10.1038/s41586-
581 020-2649-2
582 52. Seabold S, Perktold J. Statsmodels: Econometric and Statistical Modeling with Python.
583 Proc 9th Python Sci Conf. 2010;7(1): 92–96. doi:10.25080/majora-92bf1922-011
584 53. Virtanen P, Gommers R, Oliphant TE, Haberland M, Reddy T, Cournapeau D, et al. SciPy
585 1.0: fundamental algorithms for scientific computing in Python. Nat Methods. 2020;17(3):
586 261–272. doi:10.1038/s41592-019-0686-2
587 54. Dong Z, He Y, Ren Y, Wang G, Chu D. Seasonal and Year-Round Distributions of
588 Bactrocera dorsalis (Hendel) and Its Risk to Temperate Fruits under Climate Change.
589 Insects. 2022;13(6): 550. doi:10.3390/INSECTS13060550
590 55. Wijekoon WMCD, Ganehiarachchi GASM, Wegiriya HCE, Vidanage SP. Seasonal
591 forecasting of Bactrocera dorsalis Hendel, 1912 (Diptera: Tephritidae) in bioclimatic zones

of Sri Lanka using the SARIMA model. CABI Agric Biosci. 2024;5(1): 40. doi:10.1186/S43170-024-00241-2

56. Michel A, Dongmo K, Fiaboe KKM, Kekeunou S, Nanga SN, Kuate AF, et al. Temperature-based phenology model to predict the development, survival, and reproduction of the oriental fruit fly Bactrocera dorsalis. J Therm Biol. 2021;97: 102877. doi:10.1016/J.JTHERBIO.2021.102877
57. Salum JK, Mwatawala MW, Kusolwa PM, Meyer MD. Demographic parameters of the two main fruit fly (Diptera: Tephritidae) species attacking mango in Central Tanzania. J Appl Entomol. 2014;138(6): 441–448. doi:10.1111/JEN.12044
58. De Meyer M, Robertson MP, Mansell MW, Ekesi S, Tsuruta K, Mwaiko W, et al. Ecological niche and potential geographic distribution of the invasive fruit fly Bactrocera invadens (Diptera, Tephritidae). Bull Entomol Res. 2010;100(1): 35–48. doi:10.1017/S0007485309006713
59. Mayamba A, Nankinga CK, Isabirye B, Akol AM. Seasonal population fluctuations of Bactrocera invadens (Diptera: Tephritidae) in relation to mango phenology in the Lake Victoria Crescent, Uganda. Fruits. 2014;69(6): 473–480. doi:10.1051/FRUITS/2014033
60. Diatta P, Rey JY, Vayssières JF, Diarra K, Coly EV, Lechaudel M, et al. Fruit phenology of citruses, mangos and papayas influences egglaying preferences of Bactrocera invadens (Diptera: Tephritidae). Fruits. 2013;68(6): 507–516. doi:10.1051/FRUITS/2013093
61. Cugala D, Ekesi S, Ambasse D, Adamu RS, Mohamed SA. Assessment of ripening stages of Cavendish dwarf bananas as host or non-host to Bactrocera invadens. J Appl Entomol. 2014;138(6): 449–457. doi:10.1111/JEN.12045

62. Ndiaye O, Vayssières JF, Yves Rey J, Ndiaye S, Diedhiou PM, Ba CT, et al. Seasonality and range of fruit fly (Diptera Tephritidae) host plants in orchards in Niayes and the Thies Plateau (Senegal). Fruits. 2012;67(5): 311–331. doi:10.1051/FRUITS/2012024

63. Dominiak BC, Hoskins JL. Managing Oriental fruit fly, Bactrocera dorsalis (Hendel): prioritising host plants using the host reproduction number. Int J Trop Insect Sci. 2025;45(3): 1249–1275. doi:10.1007/S42690-025-01514-7

64. Manrakhan A, Verykouki E, Serfontein L, Goldshtein E, Beck RR, Kriticos DJ, et al. Temporal and spatial patterns of Bactrocera dorsalis (Diptera: Tephritidae) populations in its southern limits of distribution. Bull Entomol Res. 2025;115(5): 644–659. doi:10.1017/S0007485325100230

65. Motswagole R, Gotcha N, Nyamukondiwa C. Thermal Biology and Seasonal Population Abundance of Bactrocera dorsalis Hendel (Diptera: Tephritidae): Implications on Pest Management. Int J Insect Sci. 2019;11: 1179543319863417. doi:10.1177/1179543319863417

66. Mwatawala MW, Mziray H, Malebo H, De Meyer M. Guiding farmers' choice for an integrated pest management program against the invasive Bactrocera dorsalis Hendel (Diptera: Tephritidae) in mango orchards in Tanzania. Crop Prot. 2015;76: 103–107. doi:10.1016/j.cropro.2015.07.001

67. Mze Hassani I, Raveloson-Ravaomanarivo LH, Delatte H, Chiroleu F, Allibert A, Nouhou S, et al. Invasion by Bactrocera dorsalis and niche partitioning among tephritid species in Comoros. Bull Entomol Res. 2016;106(6): 749–758. doi:10.1017/S0007485316000456

635 68. Duyck PF, David P, Quilici S. A review of relationships between interspecific competition
636 and invasions in fruit flies (Diptera: Tephritidae). Ecol Entomol. 2004;29(5): 511–520.
637 doi:10.1111/J.0307-6946.2004.00638.X
638 69. Satarkar VR, Krishnamurthy SV, Faleiro JR, Verghese A. Spatial distribution of major
639 Bactrocera fruit flies attracted to methyl eugenol in different ecological zones of Goa, India.
640 Int J Trop Insect Sci. 2009;29(4): 195–201. doi:10.1017/S174275840999035X

641 # Supporting Information

642 **S1 Fig.** Phenological stages of six key host fruit species and *B. dorsalis* seasonal activity at all
643 sites along the Uluguru transect. Source: adapted from Shechambo [30].

644 **S2 Fig.** Multivariate Spearman correlation matrices between FTD and weather variables at each
645 site separately (n = 38–81 per site).

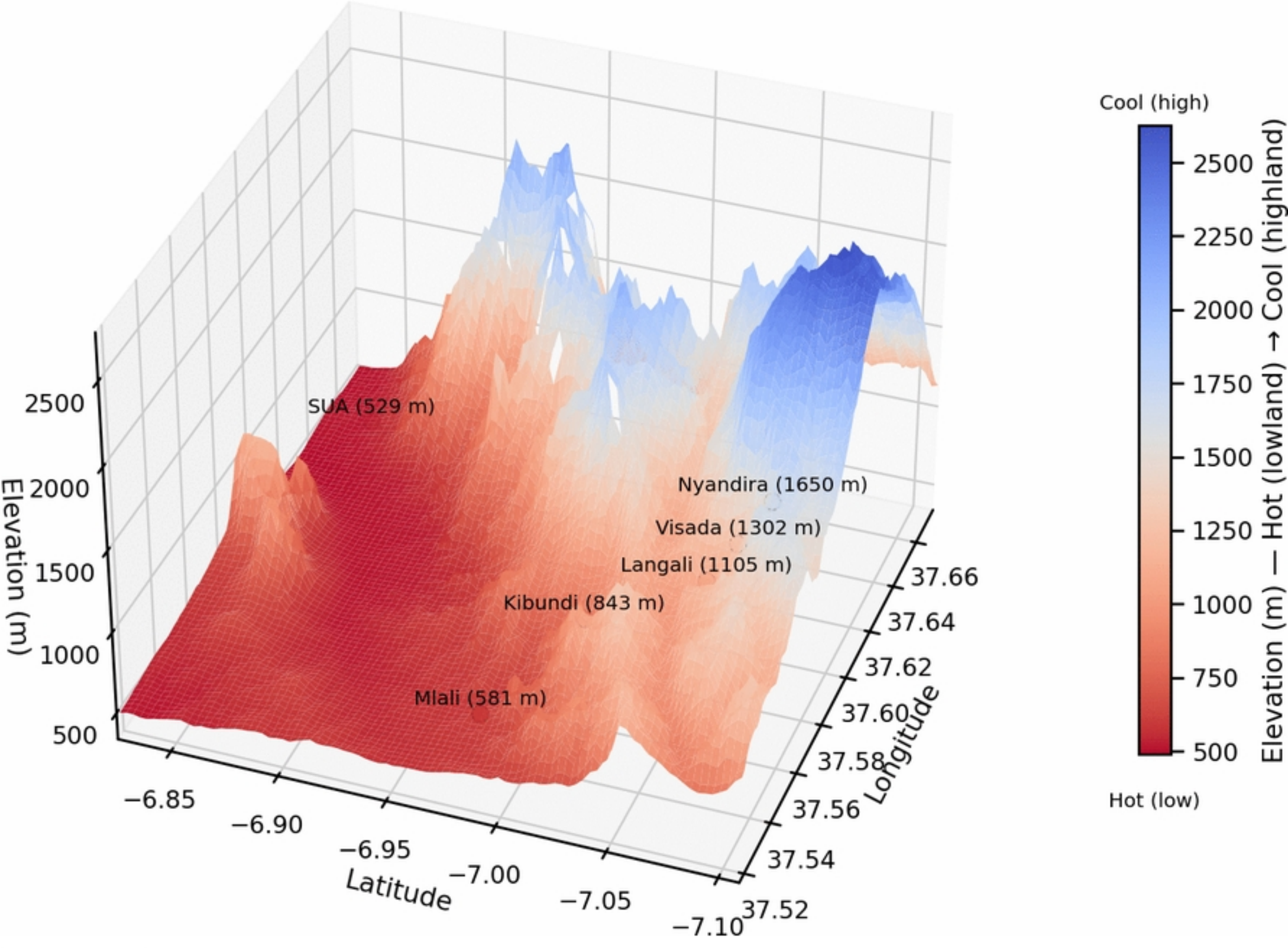
SUA (529 m)
Nyandira (1650 m)
Visada (1302 m)
Langali (1105 m)
Kibundi (843 m)
Mlali (581 m)
Elevation (m)
2500
2000
1500
1000
500
Latitude
−6.85
−6.90
−6.95
−7.00
−7.05
−7.10
Longitude
37.66
37.64
37.62
37.60
37.58
37.56
37.54
37.52
Cool (high)
Hot (low)
Elevation (m) — Hot (lowland) → Cool (highland)
2500
2250
2000
1750
1500
1250
1000
750
500

Figure1

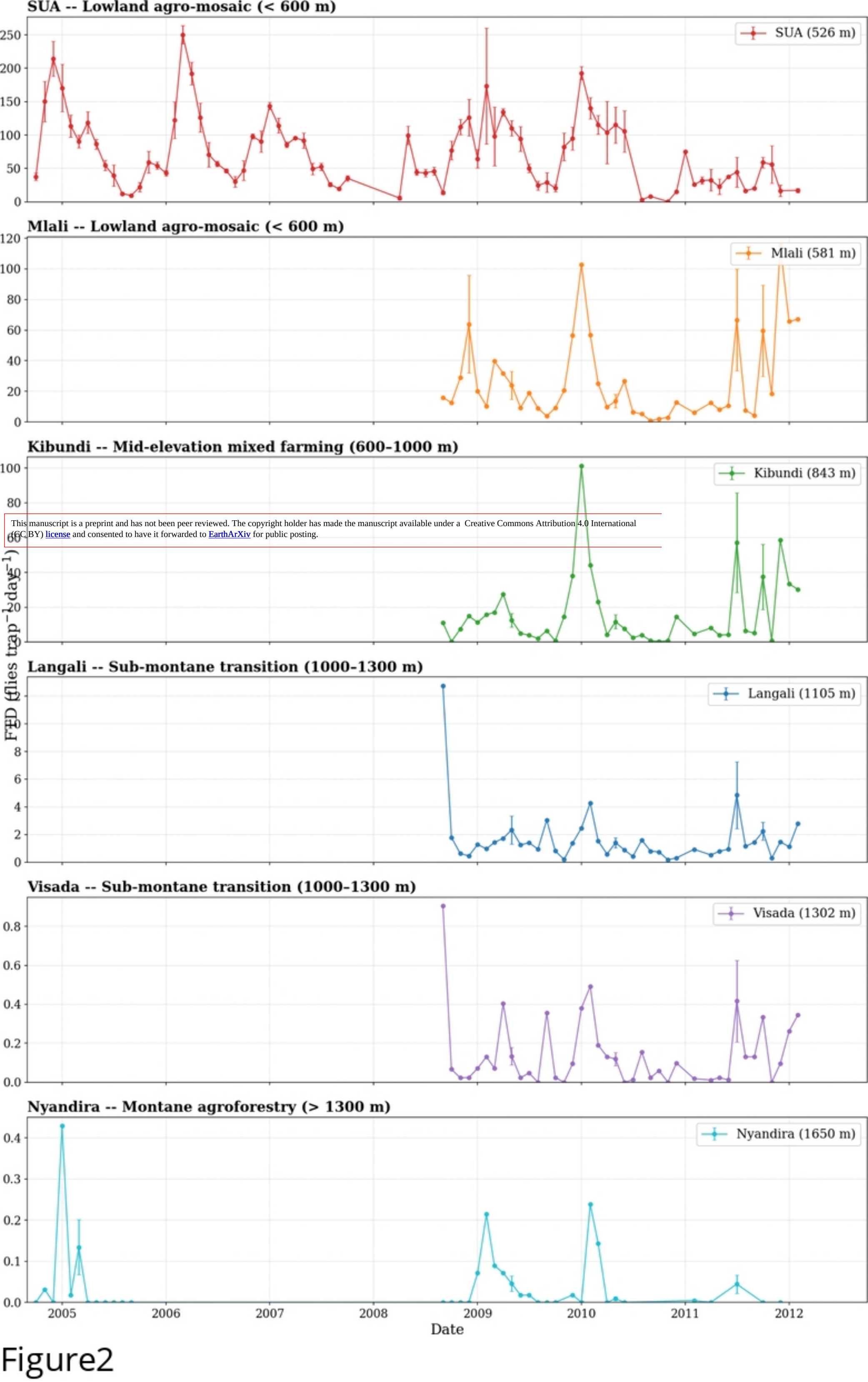

Figure2

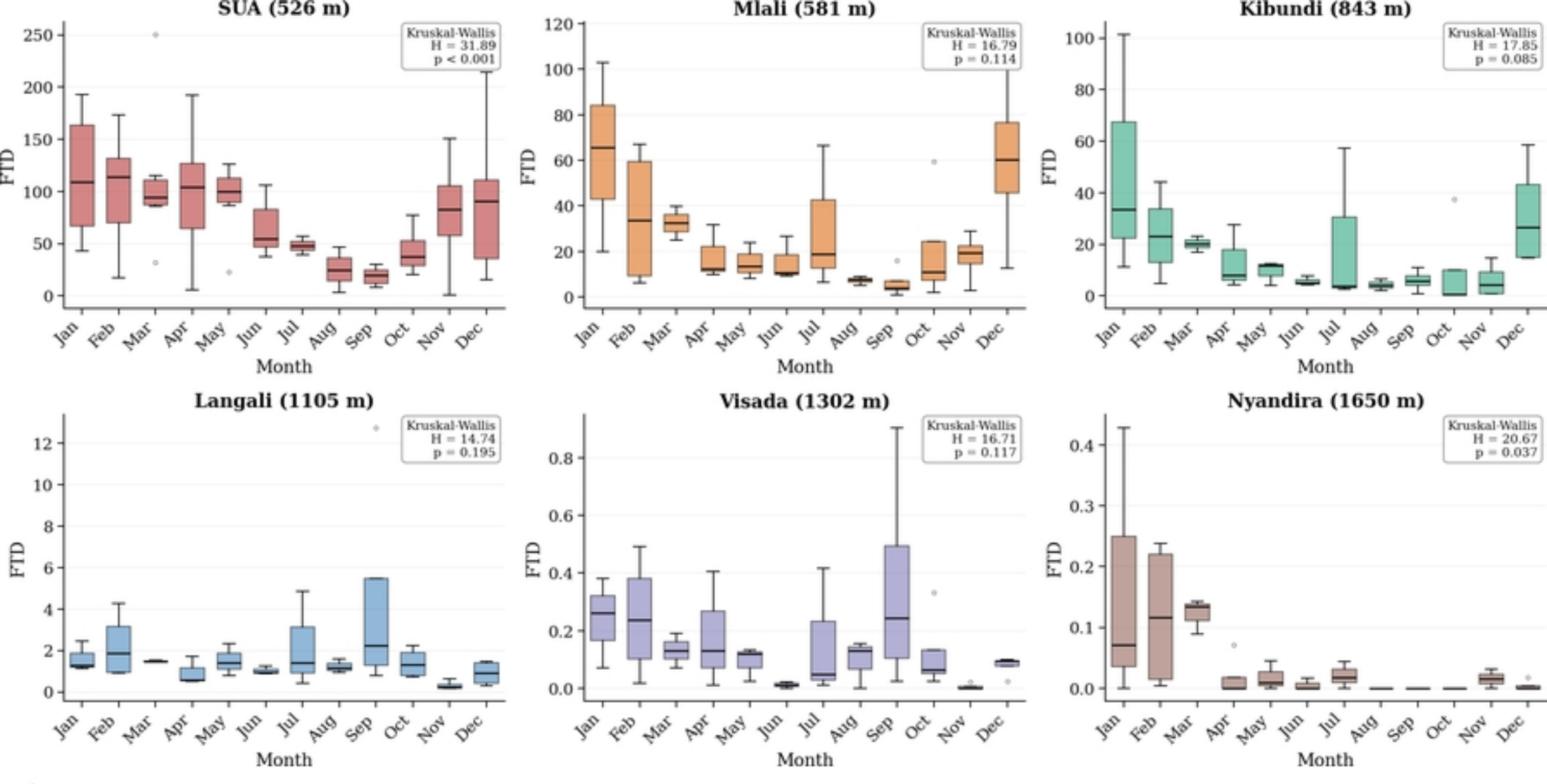
SUA (526 m)
Kruskal-Wallis
H = 31.89
p < 0.001
Mlali (581 m)
Kruskal-Wallis
H = 16.79
p = 0.114
Kibundi (843 m)
Kruskal-Wallis
H = 17.85
p = 0.085
Langali (1105 m)
Kruskal-Wallis
H = 14.74
p = 0.195
Visada (1302 m)
Kruskal-Wallis
H = 16.71
p = 0.117
Nyandira (1650 m)
Kruskal-Wallis
H = 20.67
p = 0.037
FTD
Month
Jan
Feb
Mar
Apr
May
Jun
Jul
Aug
Sep
Oct
Nov
Dec

Figure3

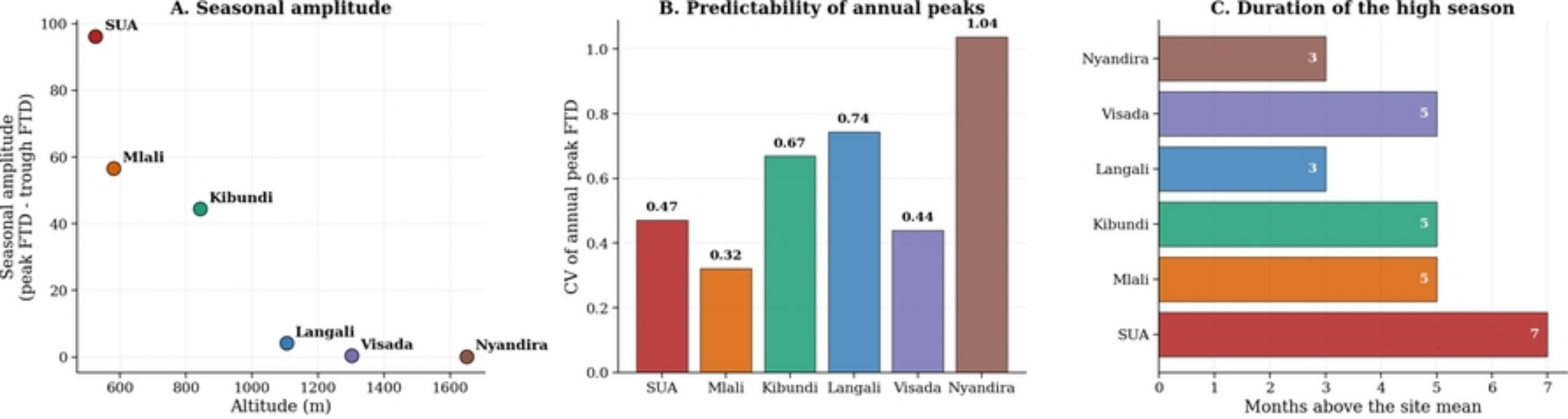
A. Seasonal amplitude
Seasonal amplitude (peak FTD - trough FTD)
Altitude (m)
SUA
Mlali
Kibundi
Langali
Visada
Nyandira
B. Predictability of annual peaks
CV of annual peak FTD
0.47
0.32
0.67
0.74
0.44
1.04
C. Duration of the high season
Months above the site mean
3
5
3
5
5
7

Figure4

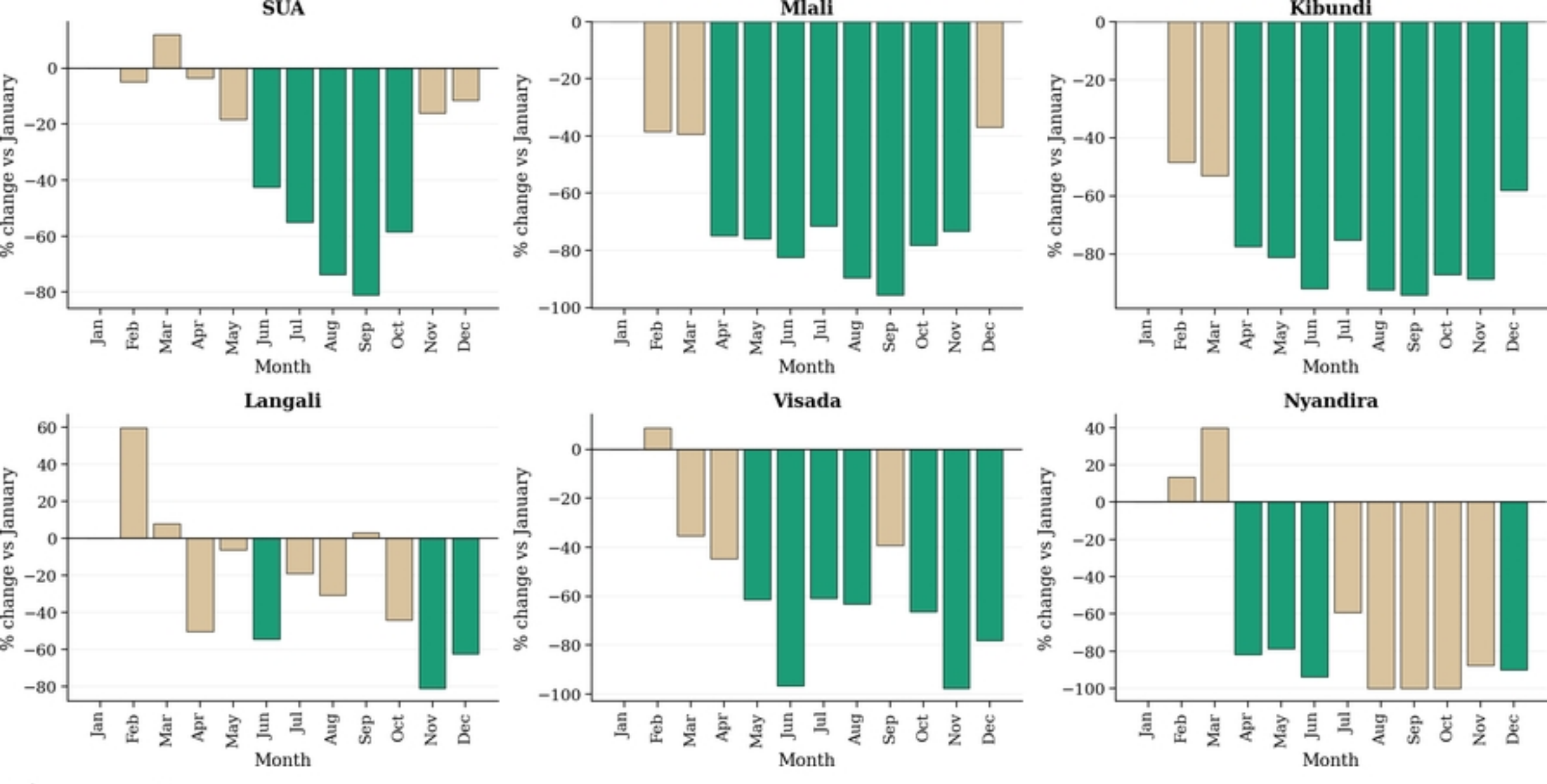
SUA
Mlali
Kibundi
Langali
Visada
Nyandira
% change vs January
Month
Jan
Feb
Mar
Apr
May
Jun
Jul
Aug
Sep
Oct
Nov
Dec

Figure5

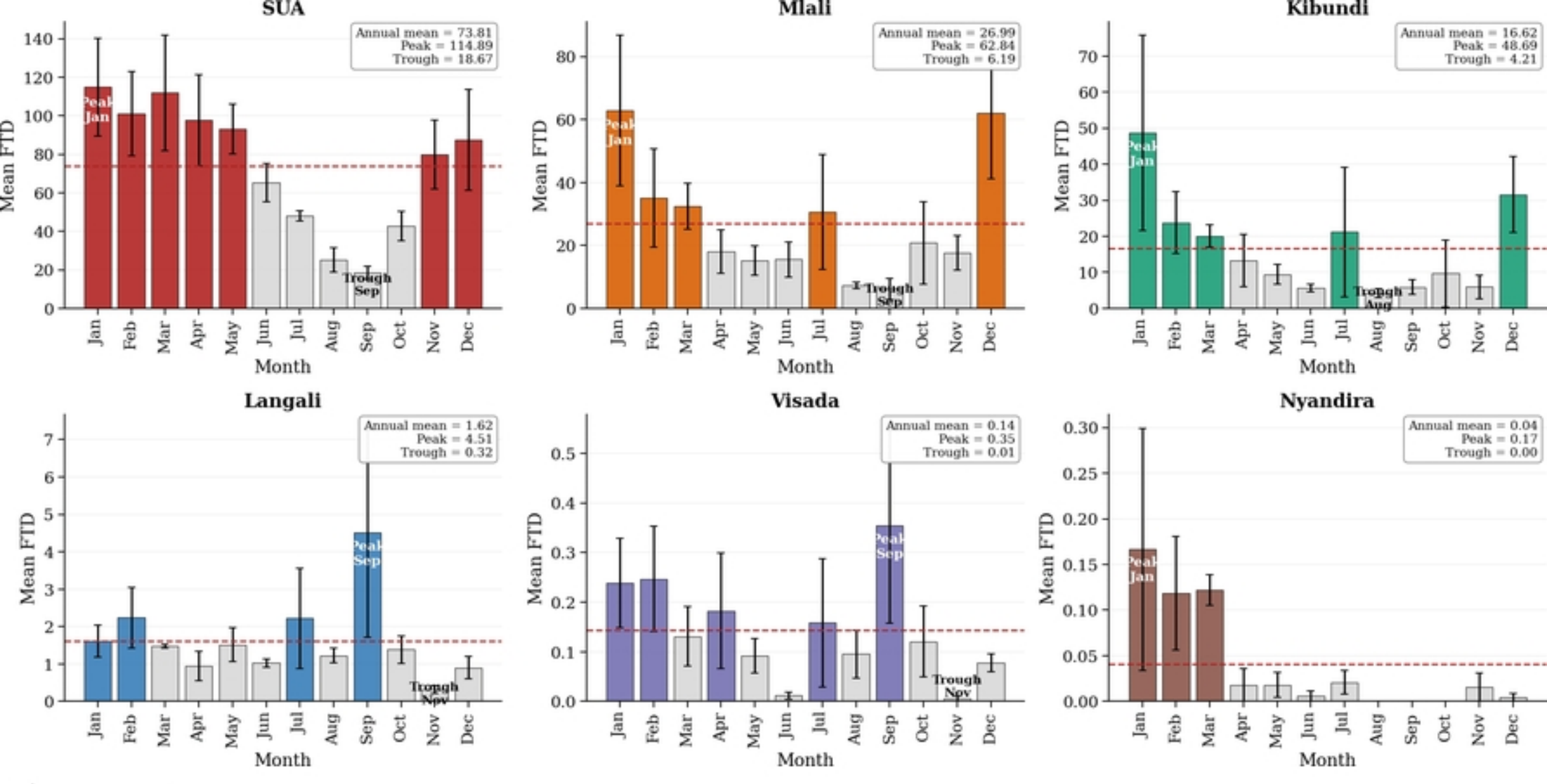
SUA
Annual mean = 73.81
Peak = 114.89
Trough = 18.67
Peak Jan
Trough Sep
Mlali
Annual mean = 26.99
Peak = 62.84
Trough = 6.19
Peak Jan
Trough Sep
Kibundi
Annual mean = 16.62
Peak = 48.69
Trough = 4.21
Peak Jan
Trough Aug
Langali
Annual mean = 1.62
Peak = 4.51
Trough = 0.32
Peak Sep
Trough Nov
Visada
Annual mean = 0.14
Peak = 0.35
Trough = 0.01
Peak Sep
Trough Nov
Nyandira
Annual mean = 0.04
Peak = 0.17
Trough = 0.00
Peak Jan
Mean FTD
Month
Jan
Feb
Mar
Apr
May
Jun
Jul
Aug
Sep
Oct
Nov
Dec

Figure6

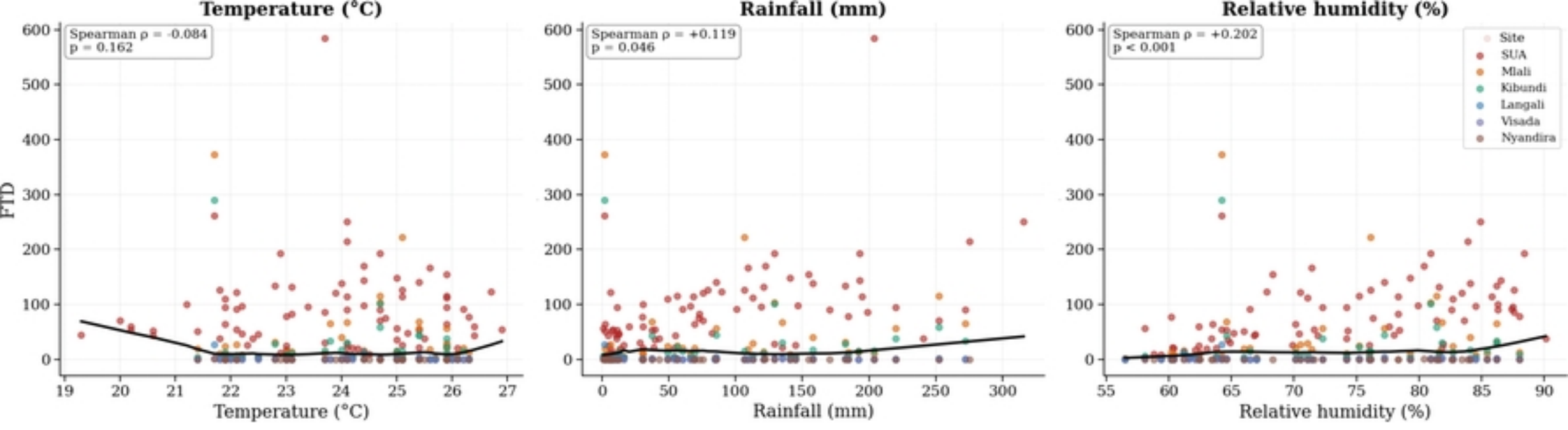
Temperature (°C)
Spearman ρ = -0.084
p = 0.162
FTD
Temperature (°C)
Rainfall (mm)
Spearman ρ = +0.119
p = 0.046
Rainfall (mm)
Relative humidity (%)
Spearman ρ = +0.202
p < 0.001
Relative humidity (%)
Site
SUA
Mlali
Kibundi
Langali
Visada
Nyandira

Figure7

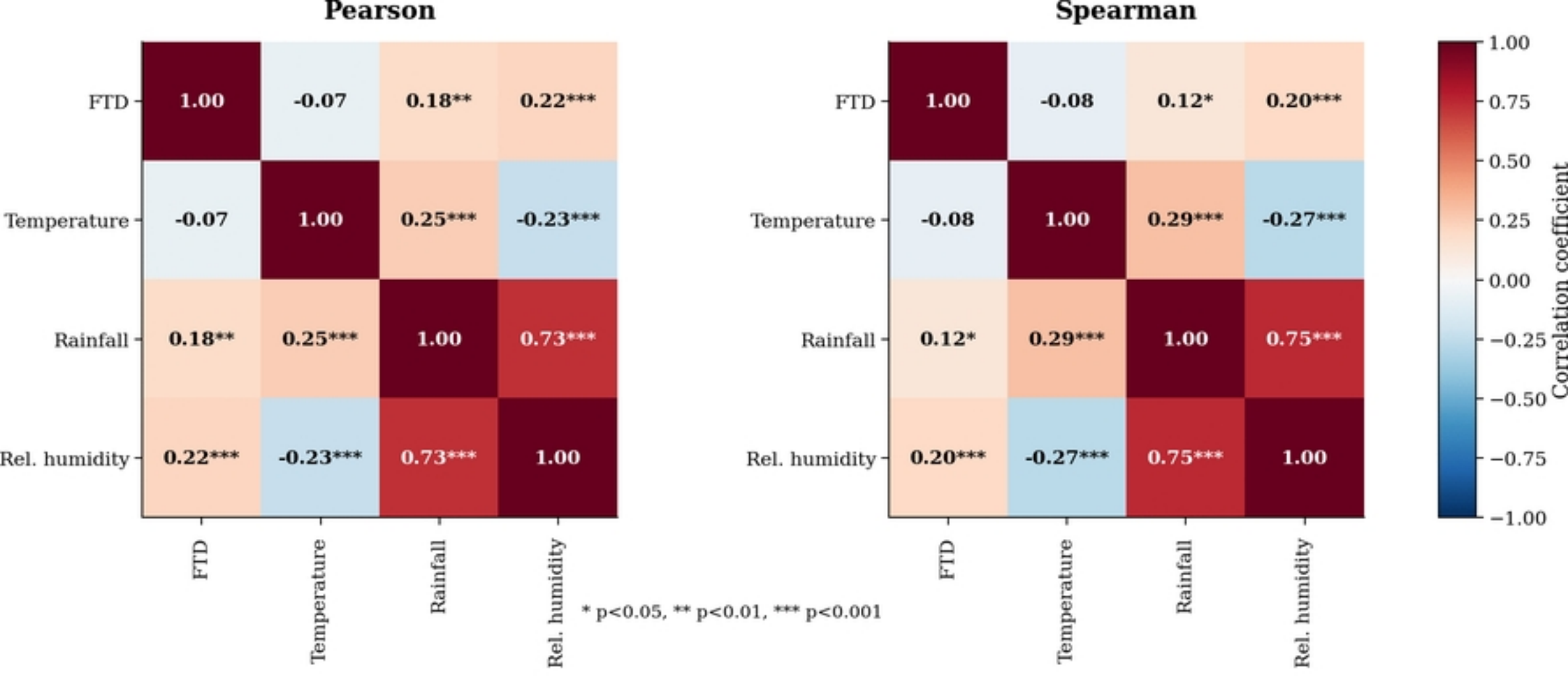
Pearson
Spearman
FTD
Temperature
Rainfall
Rel. humidity
1.00
-0.07
0.18**
0.22***
-0.07
1.00
0.25***
-0.23***
0.18**
0.25***
1.00
0.73***
0.22***
-0.23***
0.73***
1.00
-0.08
0.12*
0.20***
-0.08
0.29***
-0.27***
0.12*
0.29***
0.75***
0.20***
-0.27***
0.75***
* p<0.05, ** p<0.01, *** p<0.001
Correlation coefficient
1.00
0.75
0.50
0.25
0.00
−0.25
−0.50
−0.75
−1.00

Figure8

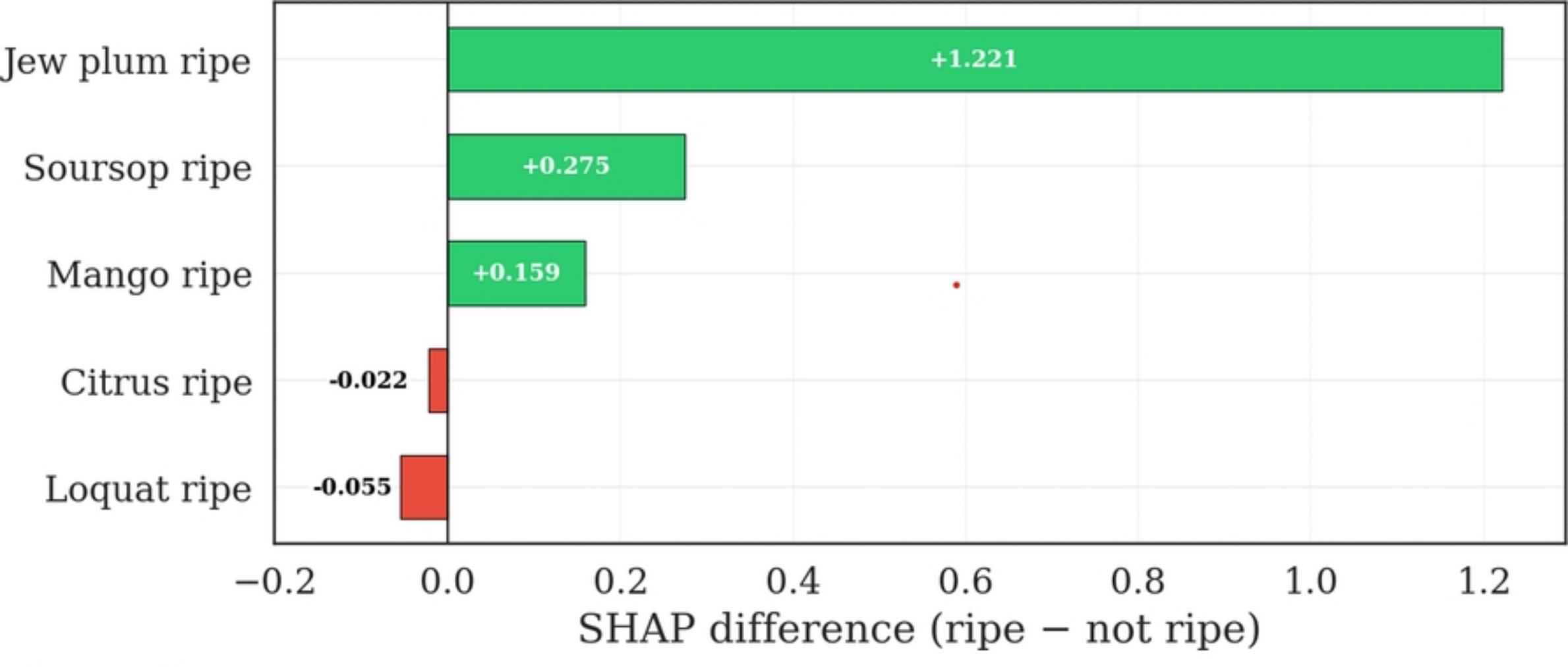
Jew plum ripe
Soursop ripe
Mango ripe
Citrus ripe
Loquat ripe
+1.221
+0.275
+0.159
-0.022
-0.055
−0.2
0.0
0.2
0.4
0.6
0.8
1.0
1.2
SHAP difference (ripe − not ripe)

Figure9

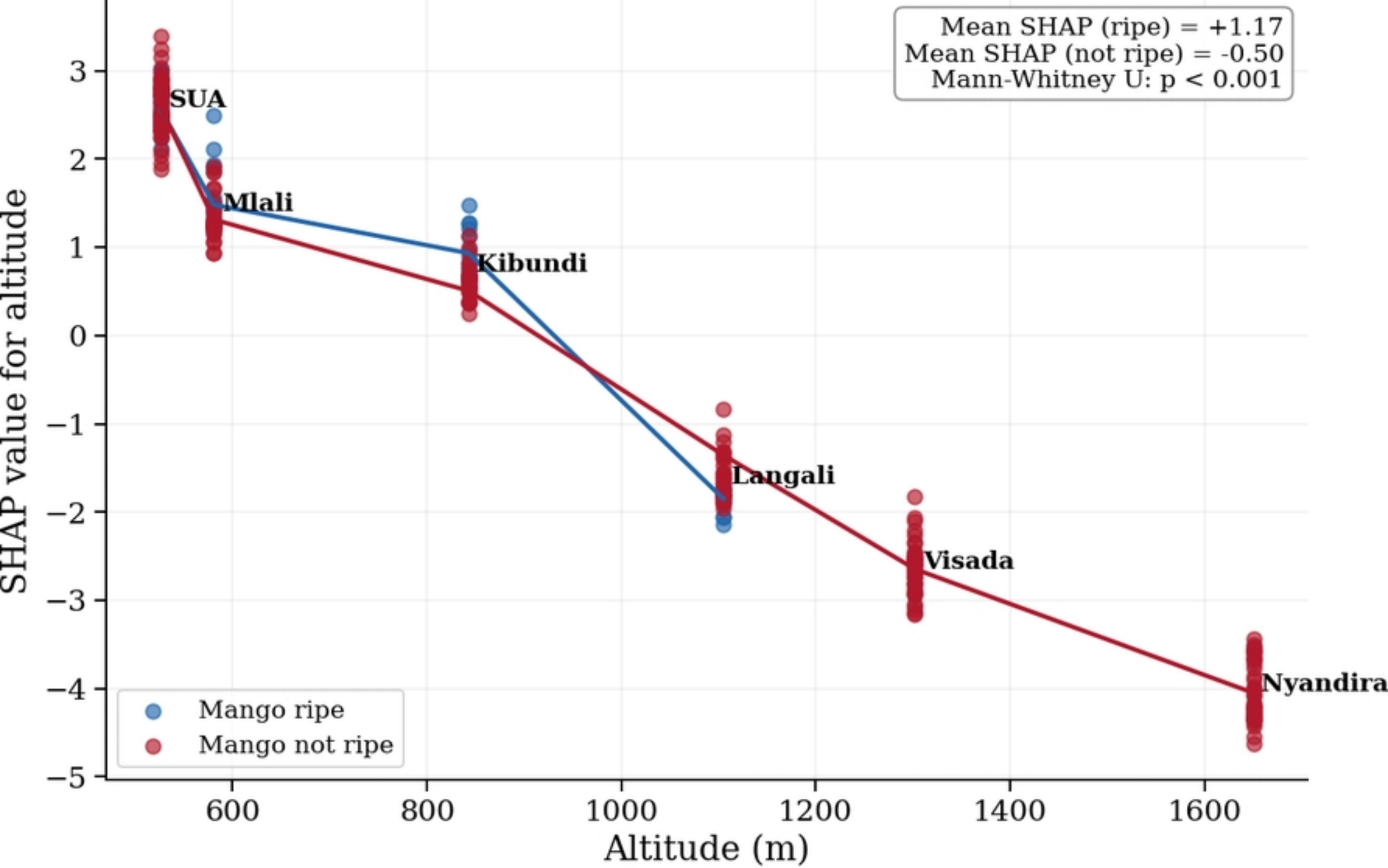
Mean SHAP (ripe) = +1.17
Mean SHAP (not ripe) = -0.50
Mann-Whitney U: p < 0.001
SUA
Mlali
Kibundi
Langali
Visada
Nyandira
Mango ripe
Mango not ripe
SHAP value for altitude
Altitude (m)
3
2
1
0
−1
−2
−3
−4
−5
600
800
1000
1200
1400
1600

Figure10

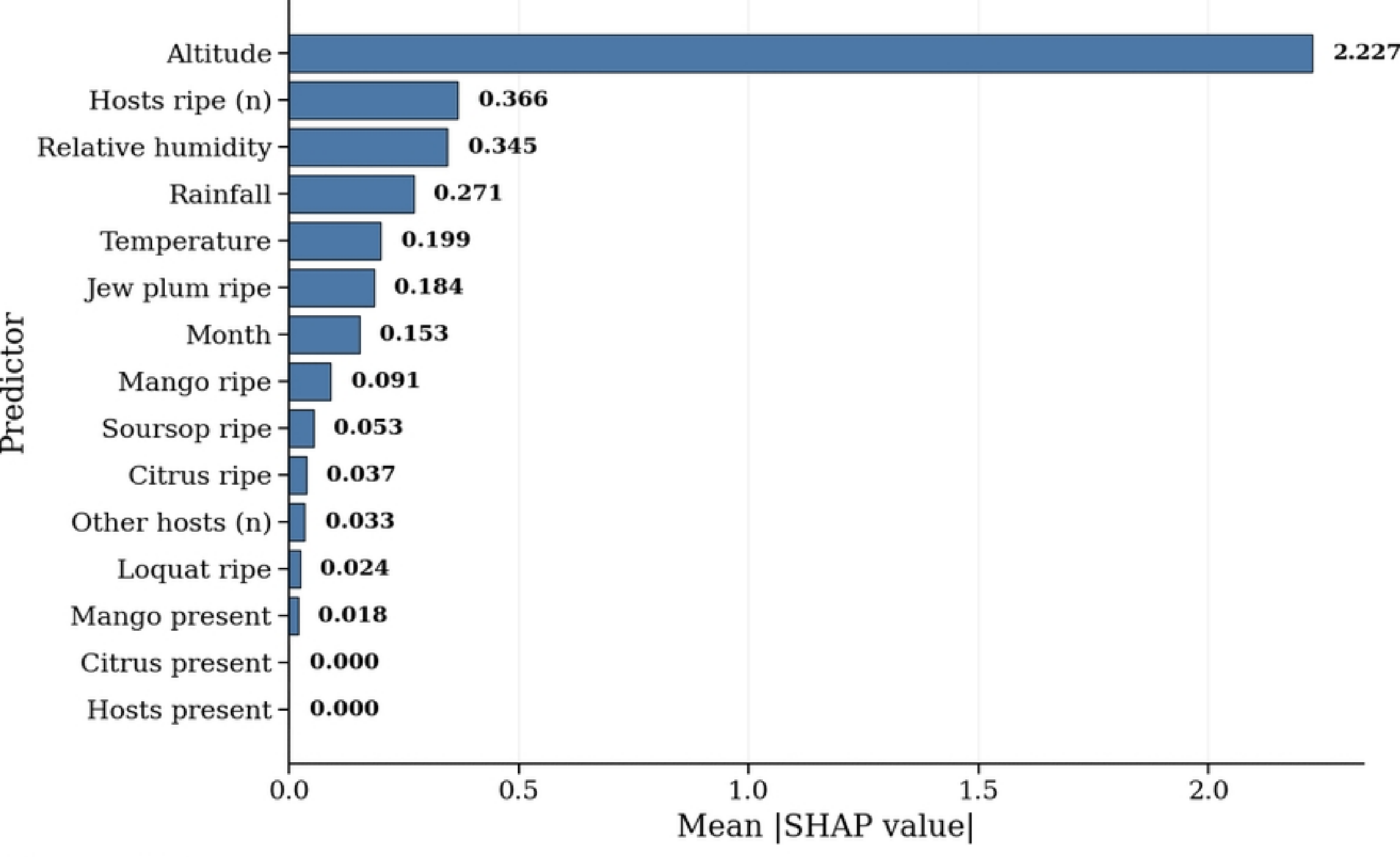
Predictor
Altitude
Hosts ripe (n)
Relative humidity
Rainfall
Temperature
Jew plum ripe
Month
Mango ripe
Soursop ripe
Citrus ripe
Other hosts (n)
Loquat ripe
Mango present
Citrus present
Hosts present
2.227
0.366
0.345
0.271
0.199
0.184
0.153
0.091
0.053
0.037
0.033
0.024
0.018
0.000
0.000
0.0
0.5
1.0
1.5
2.0
Mean |SHAP value|

Figure11


Altitude
Hosts ripe (n)
Relative humidity
Rainfall
Temperature
Jew plum ripe
Mango ripe
Soursop ripe
Citrus ripe
Loquat ripe
Predictor
Spearman | FDR <0.001
Spearman | FDR <0.001
Spearman | FDR 0.001
Spearman | FDR 0.066
Spearman | FDR 0.203
Mann-Whitney U | FDR <0.001
Mann-Whitney U | FDR <0.001
Mann-Whitney U | FDR 0.774
Mann-Whitney U | FDR <0.001
Mann-Whitney U | FDR 0.787
Reading guide:
- Lollipop length = contribution to prediction
- Point colour = FDR-adjusted support
- Labels on the right = test type and adjusted p-value
Adjusted significance
FDR < 0.001
FDR < 0.01
FDR < 0.05
Not significant
0.0
0.5
1.0
1.5
2.0
2.5
3.0
Integrated contribution score (mean |SHAP|)

Figure12